Data Collection	<LEGA-C>
Release Number	<3>
Data Provider	<Arjen van der Wel>
Date	<31.05.2021>

Abstract

We present the third data release of the Large Early Galaxy Astrophysics Census (LEGA-C), an ESO 130−night public spectroscopic survey conducted with VIMOS on the Very Large Telescope. We release >4000 spectra of galaxies mostly at 0.6 < z < 1.0, each observed for ~ 20 hours and fully reduced with a custom-built pipeline. The typical continuum S/N ≃ 17 Å for 3295 spectra of primary targets. The survey covers the 1.4 square degrees of the UltraVISTA survey in the COSMOS field (R.A. = 10h00; Dec. = +2 deg). The VIMOS high-resolution red grating is used in combination with the GG475 order separation filter, which results in a typical wavelength range of ~ 6300Å – 8800Å at a resolution of R = 2500 and a dispersion of 0.6Å per pixel.

LEGA-C's unique combination of sample size and depth enables for the first time to map the stellar content at large look-back time (8 Gigayears), across galaxies of different types and star-formation activity. Core science goals are, among others, to chart the star formation histories of galaxies, quenching of star formation, evolution of galaxy kinematics and other scaling relations. Observations started in December 2014 and were completed by March 2018.

In this release, we provide for the first time the full dataset (programs 194.A-2005 and 1100.A-0949), totaling 4081 galaxy spectra of 3741 unique galaxies, doubling the sample size with respect to the second data release in 2018. We also release a catalog with spectroscopic redshifts, emission line fluxes, Lick/IDS indices, spatially integrated stellar and gas velocity RMSs (line widths), structural parameters measured from ancillary Hubble Space Telescope imaging, and dynamical mass measurements.

Full details about the survey design, sample selection, observing strategy, data reduction, and science goals can be also found in three survey papers:

-- *"THE VLT LEGA-C SPECTROSCOPIC SURVEY: THE PHYSICS OF GALAXIES AT A LOOKBACK TIME OF 7 GYR"*: A. van der Wel et al. 2016, ApJS, 223, 29 (Hereafter referred to as W16);

-- "*THE LARGE EARLY GALAXY ASTROPHYSICS CENSUS (LEGA-C) DATA RELEASE II: DYNAMICAL AND STELLAR POPULATION PROPERTIES OF Z<1 GALAXIES IN THE COSMOS FIELD.*" C. Straatman et al. 2018, ApJS, 239, 27 (Hereafter, S18);

-- "*THE LARGE EARLY GALAXY ASTROPHYSICS CENSUS (LEGA-C) DATA RELEASE: 3500 HIGH-QUALITY SPECTRA OF Ks-SELECTED GALAXIES AT Z>0.6*": A. van der Wel et al., ApJS, submitted (Hereafter, W21)

Overview of Observations

The observations were taken from periods 94 to 100, from December 2014 to May 2018. Due to visibility constraints, most of these nights were fractional allocations to LEGA-C. Observations were conducted in visitor mode, during dark time periods, and in good weather conditions (seeing <1.3"). During sufficiently long time windows when these conditions were not achieved, the telescope was handed back to ESO staff to be used for Service Mode programs.

32 unique masks were designed and observations were organized in 15-35 Observing Blocks (OBs) of four 450 - 900 second-long exposures, depending on observing conditions. A mask was completed after ~ 20 hours depending on the conditions. No dithering was applied to avoid severe efficiency costs: dithering would sacrifice 16% − 30% in depth, equivalent to 6 − 10 hours of exposure time.

Calibrations were obtained in a non-standard manner, again to avoid a severe penalty in survey efficiency. Initially, arcs and screen flats were not taken directly after each science OB, but at the end of the (partial) night and at the average of the rotator angles of each OB observed that night. However, subsequent analysis of the full calibration dataset showed that proximity in time to the science exposures is more relevant to minimize the effects of flexure and hysteresis than the rotator angle, so our strategy was changed to taking calibration exposures every two to two and a half hours between science OBs. For short partial nights, i.e., less than two hours of allocated time, we only obtained calibration data once before or after observing the science OBs. We do not use spectrophotometric standards to flux-calibrate the spectra, but rather use the rich and well-calibrated photometric spectral energy distributions from the UltraVISTA catalog to derive the calibration.

Release Content

The LEGA-C survey was conducted in the COSMOS field (R.A. = 10hr; Dec. = +2 deg.), overlapping in area and targets with the previous redshift survey zCOSMOS (their spectroscopic redshifts were a key aspect of our sample selection approach). The R.A. - Dec. - redshift distribution of the sources is shown in Figure 1.

The primary targets are chosen from a K−band magnitude selected parent sample of ~ 10,000 galaxies with photometric redshifts z = 0.6 − 1 drawn from the UltraVISTA catalog (Muzzin, A., Marchesini, D., Stefanon, M., et al. 2013a, ApJS, 206, 8), which overlaps for the most part with the already extensively photometrically covered COSMOS field. The K−band limit ranges from K < 21.08 at z = 0.6 to K < 20.36 at z = 1.0, overall this results in a sample with a stellar mass limit of the order of ~ 10^10 solar mass. Targets for the VIMOS masks were inserted in order of K−band magnitude (brightest first) while avoiding slit collisions and independent of environment. Any remaining space in the masks was used to include 'fillers'. Ordered by priority these are 1) galaxies at z > 1 and brighter than K = 20.4; 2) galaxies at z < 1 and fainter than our K-band magnitude limit. Both of these subsamples are also ranked by K−band magnitude when designing the masks.

The sample to be released in DR3 consists of 3029 primary targets and 1052 'fillers'. DR3 comprises 4081 1-D spectra of 3741 unique galaxies (340 were included in more than one mask). The typical wavelength coverage is 6000-9000 Angstrom, with a spectral resolution of R~3500. The 20-hour integration times yielded a typical S/N = 17 (per Angstr. in the observed frame). The value-added catalog has 112 entries for each galaxy.

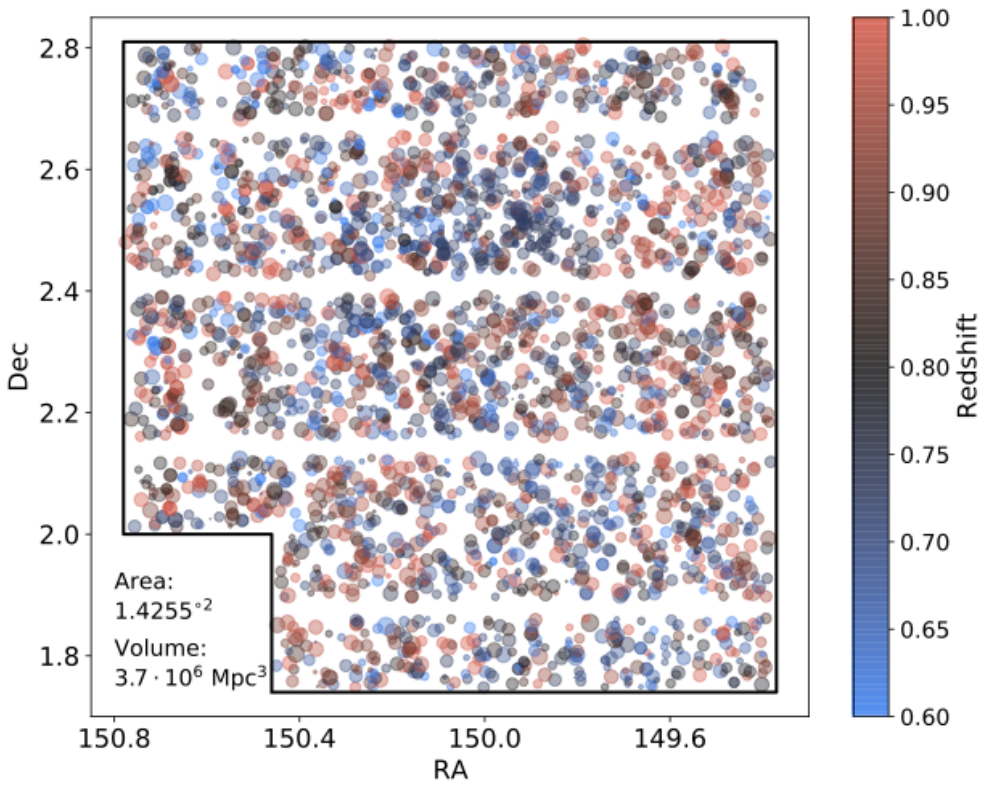

Fig 1 : Survey footprint and source distribution in the COSMOS field. Symbol size reflects the stellar velocity dispersion (see `Release Notes') in order to emphasize the more massive galaxies.

Release Notes

The spectra have a topocentric reference coordinate system, with wavelengths measured in dry air.

Data Reduction and Calibration

The raw frames were obtained from the ESO archive and processed through the recommended ESO tools at the time of observation: Reflex versions 2.7-2.8.5 (Freudling, W., Romaniello, M., Bramich, D. M., et al. 2013, A&A, 559, A96) with the VIMOS pipeline package versions 2.9.15-3.1.9.

We employ a custom pipeline to further analyze the Reflex data products. This is motivated by the need to remove bleeding of bright skylines between slits, correct for small misalign- ments between science and calibration exposures due to instrument flexure, the need for ac- curate sky-subtraction for extended objects, and optimal S/N−weighted extraction of spectra from the different OBs. An initial version of this custom pipeline was used for Data Release I and described in W16. For Data Release III a number of refinements are added, as described below, and all spectra, including those from Data Releases I and II, were processed or re-processed using the latest version of the pipeline. The custom pipeline performs the following steps.

Variance spectra are calculated from the (background + object) flux and the read noise on a pixel-by-pixel basis.

Slit definitions, i.e., the locations of sources, are verified and if necessary adjusted, with a margin at the top and bottom of the slit against bleeding of skyline flux from neighboring slits.

The location and spatial extent (FWHM) of the sources are measured by fitting a Moffat profile in the spatial direction after summing along ~800 pixels in the wavelength region between 7120 Å and 7600 Å, which is free of bright atmospheric emission lines. The location of the source is then traced along the entire wavelength range in bins of 100 pixels through a weighted fit using the variance spectrum. If there is insufficient flux to do this, the location over the entire wavelength range is assumed to be the expected location from the mask design.

We then build a galaxy+sky model for each wavelength pixel. This includes the Moffat profile as defined above at fixed location, but with the amplitude as a free parameter, and with a constant (sky) flux level as a second free parameter. To account for areas with high sky levels or large sky level gradients in the wave- length direction, e.g., near the edges of skylines, a first-order term is added to allow for a sloping background in the spatial direction.

A model for the telluric absorption features is constructed for each mask, based on a normalized blue star spectrum included in the mask. This model is adapted (in wavelength position and spectral resolution) for each galaxy to account for variations in slit alignment and spectral resolution.

Spectra from individual OBs are aligned and coadded after weighting by the S/N as measured between 7120 Å and 7600 Å.

Many galaxies have faint, extended wings in our deep spectra that are not accurately captured with the Moffat extraction kernel determined from single exposures as described above. We therefore revisit the sky sub- traction in the coadded 2D spectra, which have a much higher S/N than the single OB spectra and allow for a better as- sessment of the extended light. Summing over all wavelength pixels between 7120 Å and 7600 Å we fit a Moffat profile to the flux of the source. If this model is significantly different from the initial model we redo the source extraction + sky subtraction: keeping the shape of the new Moffat profile fixed we create a new model for sky+object for each column of pixels with the same wavelength, where we vary only the amplitude and sky back- ground (constant+slope). Third-order polynomials are then fit to the sky parameters to create a smooth master sky model which is then subtracted from the 2D spectrum and propagated into the 1D extracted spectrum by using the Moffat profile as the extraction kernel.

Emission lines trace the kinematics and spatial structure of gas, which are often different from that of the stellar continuum. For these reasons the Moffat profile that is used to characterize the spatial structure of the continuum light of a galaxy does not accurately reflect the light distribution of emission lines. As such, the sky subtraction near emission lines can be inaccurate. We identify emission lines by searching for significant peaks in smoothed 1D spectra and redo the sky+object Moffat modeling while leaving the spatial location as an additional free parameter across a 40-pixel region around the central wavelength of the emission line.

Spectra are flux calibrated using the model spectra inferred from fitting the photometric SEDs from UltraVISTA. These best-fit spectral templates for these were obtained with te Bagpipes fitting code. A 15th order polynomial is fit to the LEGA-C spectra and the ratio between the two is used to scale the LEGA-C spectra in a wavelength dependent manner. We note that the flux calibration compensates for slit losses assuming that the spectrum is the same in shape across the galaxy, but does not account for wavelength-dependent spatial gradients along the slit. We also note that in this way emission line fluxes receive the same correction, implicitly assuming slit losses are the same for the continuum and the lines.

Some sources were observed more than once over different masks. They appear as different entries in the catalog and can be distinguished by their unique identifier, which is a combination of the mask number and the ID ([mask number]_[source ID]).

Data Quality

Reduction and quality control: the output of the custom-made pipeline was visually verified on an OB-by-OB and object-by-object basis. Any problems with the slit definition, tracing, and sky subtraction were identified and, if appropriate, the pipeline was rerun. The combined 1D and 2D spectra were verified on an object-by-object basis as well.

Formal uncertainties on released quantities were derived from the variance spectra. In general, we find that those agree well with the noise level seen in the spectra themselves. Yet they do not take into account additional sources of error, such as variations in seeing or imperfect sky subtraction. The formal uncertainties were verified using the duplicate spectra. We derived factors of 1.25x to 2x larger scatter between duplicate observations and based on this applied multiplicative factors to the uncertainties released in the catalog. The uncertainties in this data release are thus final, corrected uncertainties.

Previous Releases

Data release 1

Data release2 (https://www.eso.org/qi/catalog/show/235) had 1988 spectra and the catalog 72 entries. The current data release 3 expands the number of galaxy spectra to 4081 and the catalog to 112 entries. More value-added data products were added as described below.
We note that the previous releases contained some failed spectra, such as vignetted objects, that were removed in DR3. Other sources that were removed are spectra of stars, so that LEGA-C DR3, which is a galaxy survey, only contains spectra of galaxies. These stars and catastrophic failures amount to 72 spectra (<2%).

Data Format

Files Types

The 1-d spectra files hold the spectrum in their sole binary table extensions, in four columns:

1. Wavelength, label="WAVE", unit Å, format 4-byte FLOAT

2. Flux, label "FLUX", unit 10^{19} erg s^{-1} cm^{-2} $Å^{-1}$, format 4-byte FLOAT

3. Flux error, label "ERR", unit 10^{19} erg s^{-1} cm^{-2} $Å^{-1}$, format 4-byte FLOAT 4. Quality flag, label "QUAL" (no unit), format 2-byte INTEGER

Note on flux error and quality flag: some elements in the "error" column are set to zero. This does however NOT indicate a very small error, but rather means that this element should be excluded from further analysis. Such elements show a large second derivative in the spectrum, too large to be explained by spectra features or random noise, which typically indicates the presence of a systematic imperfection in the sky subtraction at that location. For such elements, the quality flag is set to 1.

Catalogue Columns

The catalog "legac_DR3.fits" contains for each spectrum the target galaxy's object ID as well as a unique identifier combining ID and mask number, as some targets were observed more than once in different masks. It contains furthermore for each spectrum the right ascension and declination, spectroscopic redshift, stellar and gas integrated velocity dispersions, Lick/IDS indices, emission line fluxes and equivalent widths, quality flags, virial masses, and morphological quantities from the F814W image. These values are given in the file's sole binary table extension, with columns as follows:

Column	Label	Unit	Format
Target ID	OBJECT	na	4 byte long integer
Unique identifier (Mask number + target ID)	SPECT_ID	na	Ascii string
Right ascension (J2000.0)	RAJ2000	Degrees	8-byte double precision float
Declination (J2000.0)	DECJ2000	Degrees	8-byte double precision float
Filename of 1-d spectrum	Filename	na	Ascii string
Primary target flag	FLAG_PRIMARY	Na	1-byte unsigned byte
Redshift	Z	na	8-byte double precision float
Observed stellar velocity dispersion	SIGMA_STARS_PRIME	km s^{-1}	4-byte single precision float
Observed stellar velocity dispersion error	SIGMA_STARS_PRIME _ERR	km s^{-1}	4-byte single precision float
Observed gas velocity dispersion	SIGMA_GAS_PRIME	km s^{-1}	4-byte single precision float
Observed gas velocity dispersion error	SIGMA_GAS_PRIME _ERR	km s^{-1}	4-byte single precision float
LICK HD_A index	LICK_HD_A	Å	4-byte single precision float
LICK HD_A index error	LICK_HD_A_ERR	Å	4-byte single precision float
LICK HD_F index	LICK_HD_F	Å	4-byte single precision float
LICK HD_F index error	LICK_HD_F_ERR	Å	4-byte single precision float
LICK HG_A index	LICK_HG_A	Å	4-byte single precision float
LICK HG_A index error	LICK_HG_A_ERR	Å	4-byte single precision float
LICK HG_F index	LICK_HG_F	Å	4-byte single precision float
LICK HG_F index error	LICK_HG_F_ERR	Å	4-byte single precision float
LICK HB index	LICK_HB	Å	4-byte single precision float
LICK HB index error	LICK_HB_ERR	Å	4-byte single precision float
LICK CN1 index	LICK_CN1	Å	4-byte single precision float
LICK CN1 index error	LICK_CN1_ERR	Å	4-byte single precision float
LICK CN2 index	LICK_CN2	Å	4-byte single precision float
LICK CN2 index error	LICK_CN2_ERR	Å	4-byte single precision float
LICK CA4227 index	LICK_CA4227	Å	4-byte single precision float
LICK CA4227 index error	LICK_CA4227_ERR	Å	4-byte single precision float
LICK G4300 index	LICK_G4300	Å	4-byte single precision float
LICK G4300 index error	LICK_G4300_ERR	Å	4-byte single precision float
LICK FE4383 index	LICK_FE4383	Å	4-byte single precision float

LICK FE4383 index error	LICK_FE4383_ERR	Å	4-byte single precision float
LICK CA4455 index	LICK_CA4455	Å	4-byte single precision float
LICK CA4455 index error	LICK_CA4455_ERR	Å	4-byte single precision float
LICK FE4531 index	LICK_FE4531	Å	4-byte single precision float
LICK FE4531 index error	LICK_FE4531_ERR	Å	4-byte single precision float
LICK C4668 index	LICK_C4668	Å	4-byte single precision float
LICK C4668 index error	LICK_C4668_ERR	Å	4-byte single precision float
LICK FE5015 index	LICK_FE5015	Å	4-byte single precision float
LICK FE5015 index error	LICK_FE5015_ERR	Å	4-byte single precision float
LICK MG1 index	LICK_MG1	Å	4-byte single precision float
LICK MG1 index error	LICK_MG1_ERR	Å	4-byte single precision float
LICK MG2 index	LICK_MG2	Å	4-byte single precision float
LICK MG2 index error	LICK_MG2_ERR	Å	4-byte single precision float
LICK MGB index	LICK_MGB	Å	4-byte single precision float
LICK MGB index error	LICK_MG1_ERR	Å	4-byte single precision float
LICK FE5270 index	LICK_FE5270	Å	4-byte single precision float
LICK FE5270 index error	LICK_FE5270_ERR	Å	4-byte single precision float
LICK FE5335 index	LICK_FE5335	Å	4-byte single precision float
LICK FE5335 index error	LICK_FE5335_ERR	Å	4-byte single precision float
LICK FE5406 index	LICK_FE5406	Å	4-byte single precision float
LICK FE5406 index error	LICK_FE5406_ERR	Å	4-byte single precision float
LICK D4000_N index	D4000_N	Å	4-byte single precision float
LICK D4000_N index error	D4000_N_ERR	Å	4-byte single precision float
[OII]3727 emission line flux	OII_3727_FLUX	10^{19} erg s^{-1} cm^{-2} $Å^{-1}$	4-byte single precision float
[OII]3727 emission line flux error	OII_3727_ERR	10^{19} erg s^{-1} cm^{-2} $Å^{-1}$	4-byte single precision float
[OII]3727 emission line EW	OII_3727_EW	Å	4-byte single precision float
[OII]3727 emission line EW error	OII_3727_EW_ERR	Å	4-byte single precision float
[NEIII]3869 emission line flux	NEIII_3869_FLUX	10^{19} erg s^{-1} cm^{-2} $Å^{-1}$	4-byte single precision float
[NEIII]3869 emission line flux error	NEIII_3869_ERR	10^{19} erg s^{-1} cm^{-2} $Å^{-1}$	4-byte single precision float
[NEIII]3869 emission line EW	NEIII_3869_EW	Å	4-byte single precision float
[NEIII]3869 emission line EW error	NEIII_3869_EW_ERR	Å	4-byte single precision float
[HEI]3890 emission line flux	HEI_3890_FLUX	10^{19} erg s^{-1} cm^{-2} $Å^{-1}$	4-byte single precision float
[HEI]3890 emission line flux error	HEI_3890_ERR	10^{19} erg s^{-1} cm^{-2} $Å^{-1}$	4-byte single precision float
[HEI]3890 emission line EW	HEI_3890_EW	Å	4-byte single precision float
[HEI]3890 emission line EW error	HEI_3890_EW_ERR	Å	4-byte single precision float

Hδ emission line flux	Hd_FLUX	10^{19} erg s^{-1} cm^{-2} $Å^{-1}$	4-byte single precision float
Hδ emission line flux error	Hd_FLUX_ERR	10^{19} erg s^{-1} cm^{-2} $Å^{-1}$	4-byte single precision float
Hδ emission line EW	Hd_EW	Å	4-byte single precision float
Hδ emission line EW error	Hd_EW_ERR	Å	4-byte single precision float
Hγ emission line flux	Hg_FLUX	10^{19} erg s^{-1} cm^{-2} $Å^{-1}$	4-byte single precision float
Hγ emission line flux error	Hg_FLUX_ERR	10^{19} erg s^{-1} cm^{-2} $Å^{-1}$	4-byte single precision float
Hγ emission line EW	Hg_EW	Å	4-byte single precision float
Hγ emission line EW error	Hg_EW_ERR	Å	4-byte single precision float
[OIII]4363 emission line flux	OIII_4363_FLUX	10^{19} erg s^{-1} cm^{-2} $Å^{-1}$	4-byte single precision float
[OIII]4363 emission line flux error	OIII_4363_ERR	10^{19} erg s^{-1} cm^{-2} $Å^{-1}$	4-byte single precision float
[OIII]4363 emission line EW	OIII_4363_EW	Å	4-byte single precision float
[OIII]4363 emission line EW error	OIII_4363_EW_ERR	Å	4-byte single precision float
Hβ emission line flux	Hb_FLUX	10^{19} erg s^{-1} cm^{-2} $Å^{-1}$	4-byte single precision float
Hβ emission line flux error	Hb_FLUX_ERR	10^{19} erg s^{-1} cm^{-2} $Å^{-1}$	4-byte single precision float
Hβ emission line EW	Hb_EW	Å	4-byte single precision float
Hβ emission line EW error	Hb_EW_ERR	Å	4-byte single precision float
[OIII]4959 emission line flux	OIII_4959_FLUX	10^{19} erg s^{-1} cm^{-2} $Å^{-1}$	4-byte single precision float
[OIII]4959 emission line flux error	OIII_4959_ERR	10^{19} erg s^{-1} cm^{-2} $Å^{-1}$	4-byte single precision float
[OIII]4959 emission line EW	OIII_4959_EW	Å	4-byte single precision float
[OIII]4959 emission line EW error	OIII_4959_EW_ERR	Å	4-byte single precision float
[OIII]5007 emission line flux	OIII_5007_FLUX	10^{19} erg s^{-1} cm^{-2} $Å^{-1}$	4-byte single precision float
[OIII]5007 emission line flux error	OIII_5007_ERR	10^{19} erg s^{-1} cm^{-2} $Å^{-1}$	4-byte single precision float
[OIII]5007 emission line EW	OIII_5007_EW	Å	4-byte single precision float
[OIII]5007 emission line EW error	OIII_5007_EW_ERR	Å	4-byte single precision float
F814W Half-light radius along the major axis	SERSIC_RE	Arcsecond	4-byte single precision float
F814W Half-light radius along the major axis error	SERSIC_RE_ERR	Arcsecond	4-byte single precision float
F814W Sérsic index	SERSIC_N	na	4-byte single precision float
F814W Sérsic index error	SERSIC_N_ERR	na	4-byte single precision float
F814W axis ratio	SERSIC_Q	na	4-byte single precision float
F814W axis ratio error	SERSIC_Q_ERR	na	4-byte single precision float
F814W major axis position angle	SERSIC_PA	Degree	4-byte single precision float
F814W major axis position angle error	SERSIC_PA_ERR	Degree	4-byte single precision float
F814W magnitude	SERSIC_MAG	AB magnitude	4-byte single precision float
F814W magnitude error	SERSIC_MAG_ERR	AB magnitude	4-byte single precision float

GALFIT limit flag (0: good; 1: fit converged to parameter limits)	SERSIC_LIMIT	na	4-byte single precision float
Inclination corrected stellar velocity dispersion	SIGMA_STARS_VIR	km s^{-1}	4-byte single precision float
Inclination corrected stellar velocity dispersion error	SIGMA_STARS_VIR _ERR	km s^{-1}	4-byte single precision float
Logarithm of virial mass	LOG_M_VIR	Solar mass	4-byte single precision float
Logarithm of virial mass error	LOG_M_VIR_ERR	Solar mass	4-byte single precision float
Overall median S/N per pixel	SN	$pixel^{-1}$	4-byte single precision float
S/N at rest-frame 4000 Å	SN_RF_4000	$pixel^{-1}$	4-byte single precision float
S/N at observed-frame 8030 Å	SN_OBS_8030	$pixel^{-1}$	4-byte single precision float
total completeness correction	TCOR	na	4-byte single precision float
sample completeness correction	SCOR	na	4-byte single precision float
volume completeness correction	VCOR	na	4-byte single precision float
morphology flag (0: good; 1: unresolved multiple or irregular; 2: secondary at different z)	FLAG_MORPH	Na	1-byte unsigned byte
spectroscopy flag (0: good; 1: mid-IR/X-ray AGN; 2: photometric flux calibration error)	FLAG_SPEC	Na	1-byte unsigned byte

Acknowledgements

Please cite the following papers when using these data:

-- *"THE VLT LEGA-C SPECTROSCOPIC SURVEY: THE PHYSICS OF GALAXIES AT A LOOKBACK TIME OF 7 GYR"*: A. van der Wel et al. 2016, ApJS, 223, 29;

-- "*THE LARGE EARLY GALAXY ASTROPHYSICS CENSUS (LEGA-C) DATA RELEASE: 3500 HIGH-QUALITY SPECTRA OF Ks-SELECTED GALAXIES AT Z>0.6*": A. van der Wel et al., ApJS, submitted

Please use the following statement in your articles when using these data:

"Based on data products from observations made with ESO Telescopes at the La Silla Paranal Observatory under programme IDs 194A.2005 and 1100.A-0949 (The LEGA-C Public Spectroscopy Survey). The LEGA-C project has received funding from the European Research Council (ERC) under the European Union's Horizon 2020 research and innovation programme (grant agreement No. 683184). "